Available online at www.sciencedirect.com
SCIENCE DIRECT
Journal of Molecular Spectroscopy 237 (2006) 11–18
Journal of MOLECULAR SPECTROSCOPY
www.elsevier.com/locate/jms

Near infrared emission spectra of CoH and CoD

Iouli E. Gordon [a], Robert J. Le Roy [b], Peter F. Bernath [a,b,*]

[a] Department of Physics, University of Waterloo, Waterloo, Ont., Canada N2L 3G1
[b] Department of Chemistry, University of Waterloo, Waterloo, Ont., Canada N2L 3G1

Received 8 December 2005; in revised form 9 February 2006
Available online 6 March 2006

Abstract

New high resolution emission spectra of CoH and CoD molecules have been recorded in the 640 nm to 3.5 μm region using a Fourier transform spectrometer. The bands were excited in a carbon tube furnace by the reaction of cobalt metal vapor and a mixture of H_2 or D_2 with He at a temperature of about 2600 °C. Eight bands were observed for the $A'^3\Phi_4$–$X^3\Phi_4$ electronic transition of CoD, and five bands for the corresponding transition of CoH. The (0,0) bands of the $A'^3\Phi_3$–$X^3\Phi_3$ system were also recorded for both isotopologues, although one of the parity components in the $X^3\Phi_3$ sub-state of CoH was found to be perturbed. The $A'^3\Phi_3$–$X^3\Phi_4$ transition was also observed in our spectrum of CoH. In addition, a new [13.3]4 electronic state was found by observing [13.3]4–$X^3\Phi_3$ and [13.3]4–$X^3\Phi_4$ transitions in the spectrum of CoD. Analysis of the transitions with $\Delta\Omega = 0, \pm 1$ provided more accurate values of spin–orbit splittings between $\Omega = 4$ and $\Omega = 3$ components. The ground-state data for both molecules were fitted both to band-constant and Dunham-expansion expressions, and a combined-isotopologue analysis of the $X^3\Phi_4$ spin component was carried out using the data for CoH and CoD. The upper states were represented by term values in these analyses because of perturbations, but estimated band constants for them were obtained in separate fits in which ground-state constants were held fixed.

Keywords: Cobalt monohydride; Fourier transform spectroscopy; Near infrared; Spin–orbit splitting

1. Introduction

Molecules containing 3*d*-transition metal atoms usually have many low-lying electronic states with complex structure, due to their unfilled *d*-shells, and their electronic spectra are complicated because of the perturbations caused by interactions of close-lying electronic states. Spectra of the cobalt-containing molecules such as cobalt monohydride are a perfect example of such complexity.

The first observation of the electronic spectra of CoH was reported by Heimer in 1937 [1]. The spectra were recorded in emission from a King furnace (carbon tube furnace), and Heimer was able to assign two of the observed bands (at 420.3 and 449.2 nm) as the (1,0) and (0,0) bands of the $A^3\Phi_4 \rightarrow X^3\Phi_4$ transition. Despite a suggestion in [2] (based on the electronic configuration proposed in [1]) that the ground electronic state of CoH should be a $^1\Gamma$ state, it was proved in subsequent work that it is in fact a $^3\Phi$ state. Klynning and co-workers [3–6] significantly extended Heimer's results for the *A*–*X* transition by recording the (1,1) band of CoH and several bands of the corresponding system of CoD. In these experiments, they were also able to observe the (0,0) transition between $\Omega'' = \Omega' = 3$ spin components for CoH and the analogous (0,0) and (1,0) bands of CoD. However, only one parity component of the $\Omega = 3$ transitions was observed for CoH. Smith [7] was also able to see some of these transitions in absorption behind reflected shock waves.

Varberg et al. [8,9] later recorded several new bands by laser excitation spectroscopy. Two of the analyzed $\{\Omega' = 4\}$–$X^3\Phi_4$ transitions were later identified by Barnes et al. [10] as the (3,0) and (4,0) bands of the $A'^3\Phi_4$–$X^3\Phi_4$ electronic transition. Varberg et al. [8] had also observed resolved fluorescence from an excited [16.0]3 state, which enabled them to find a new electronic state (presumably

* Corresponding author. Fax: +1 519 746 0435.
E-mail address: bernath@uwaterloo.ca (P.F. Bernath).

0022-2852/$ - see front matter © 2006 Elsevier Inc. All rights reserved.
doi:10.1016/j.jms.2006.02.011

$^3\Delta_3$) lying 2469 cm^{-1} above $X^3\Phi_4$, as well as to determine that the spin–orbit splitting between the $\Omega'' = 4$ and 3 spin components is 728 (±3) cm^{-1}. A little later, Barnes et al. [10] carried out laser excitation experiments on CoH and CoD generated in a laser ablation/molecular beam source, and recorded the (0,0) to (5,0) bands of the $A'^3\Phi_4$–$X^3\Phi_4$ electronic transition. The (0,0) bands were recorded at high resolution, and a hyperfine analysis was carried out for both molecules. The electron configuration of the $A'^3\Phi$ state was found to be $(7\sigma)^1(3d\delta)^3(3d\pi)^3(8\sigma)^1$. In addition, Barnes et al. carried out resolved fluorescence experiments and determined the spin–orbit splitting in the ground state of the CoD molecule.

The $A'^3\Phi$–$X^3\Phi$ transition in CoH was also studied by Ram et al. [11] in emission using a Fourier transform spectrometer. For the $A'^3\Phi_4$–$X^3\Phi_4$ electronic transition the (0,0) and (0,1) bands were observed, while the (0,0) band was observed for the $A'^3\Phi_3$–$X^3\Phi_3$ transition, although one of its parity components was missing as it had been in [6]. Photoelectron spectroscopy of CoH^- [12] showed the existence of an excited electronic state of quintet multiplicity lying 0.8 eV above the ground state of CoH. The ground $X^3\Phi$ electronic state of CoH was also studied by laser magnetic resonance (LMR). In particular, Lipus et al. [13] reported the infrared spectrum of the fundamental band of the $X^3\Phi_4$ sub-state, and Beaton et al. [14,15] carried out far-infrared LMR experiments and performed a hyperfine analysis of the $X^3\Phi_4$ and $X^3\Phi_3$ sub-states.

The first theoretical work on CoH was reported by Chong et al. [16], who predicted some spectroscopic parameters for the ground $X^3\Phi$ state using the modified coupled-pair functional (MCPF) method. Anglada et al. [17] carried out calculations which focussed on the low-lying electronic states of CoH^+, but they also calculated the ionization potential for the $X^3\Phi$ state of CoH. A set of very thorough ab initio calculations was performed by Freindorf et al. [18], who studied 30 electronic states of singlet, triplet and quintet multiplicity lying within 4 eV of the ground state. In 1997, Barone and Adamo [19] calculated some properties of CoH and other first-row transition metal hydrides to test a new density functional method. Schultz et al. [20] included CoH into their metal-ligand bond energy database, which is used for testing existing density functionals and developing new ones. Theoretical calculations on the CoH molecule are also currently in progress in the group of Hirano [21].

None of the aforementioned experimental studies were able to locate the $\Omega = 2$ spin component for the ground state or for any of the observed excited electronic states. Also $\Delta\Omega = \pm 1$ transitions were not observed at high resolution, and there was not enough vibrational data to allow a combined-isotopologue fit of data for CoH and CoD. It was therefore decided to revisit the $A'^3\Phi$–$X^3\Phi$ system to obtain the missing information.

In this paper, we report the analysis of numerous bands of CoH and CoD in the near infrared region. This work significantly extends the available vibrational and rotational information for the $A'^3\Phi$ and $X^3\Phi$ electronic states, allowing us to perform Dunham-type and combined-isotopologue fits. The $\Delta\Omega = -1$ transition was also observed and analyzed for CoH. In addition, new [13.3]4–$X^3\Phi_3$ and [13.3]4–$X^3\Phi_4$ transitions were observed for CoD.

2. Experimental details

About 40 g of cobalt metal was heated in a King furnace to a temperature of ~2600 °C with a mixture of hydrogen (or deuterium) and helium gases flowing slowly through the system. The total pressure inside the furnace was kept between 150 and 200 Torr. It was found that the use of argon instead of helium allows higher temperatures to be achieved, but can be harmful to the carbon heating element. A BaF_2 lens was employed to image emission from the King furnace onto the entrance aperture of a Bruker IFS 120 HR Fourier transform spectrometer.

The CoH/D emission spectra were recorded in two parts. The 8000–15 700 cm^{-1} region was recorded using a silicon photodiode detector, quartz beamsplitter and 640 nm red pass optical filter that blocked the signal from the He–Ne laser of the spectrometer. The 1800–10 000 cm^{-1} region was recorded using a CaF_2 beamsplitter and an InSb detector cooled with liquid nitrogen. A total of 100–200 scans (depending on the experiment) were co-added at a resolution of 0.05 cm^{-1} to obtain a good signal-to-noise ratio (S/N). An overview spectrum of CoD in the near infrared region is shown in Fig. 1. To display the bands more clearly, the baseline was corrected by eliminating the blackbody emission profile using the Bruker OPUS program.

Line positions were measured using a Windows-based program called WSpectra, written by M. Carleer (Université Libre de Bruxelles). The widths of the individual lines in different bands vary from 0.05 to 0.8 cm^{-1}. In addition to Doppler and pressure broadening, the lines are broadened by unresolved hyperfine and Ω-doubling splittings. Significant broadening due to hyperfine structure (^{59}Co has a large nuclear spin, $I = \frac{7}{2}$, and a large magnetic moment, $\mu = 4.627$ nuclear magnetons) is present, not only in the lower J lines, but also for some higher J lines of the transitions terminating on the $\Omega = 3$ component of the ground $X^3\Phi$ state (see discussion). The CoH spectrum in the 8000–15 700 cm^{-1} region was calibrated using lines reported in [11]. The corresponding spectrum of CoD was calibrated using lines arising from impurities common to the spectra of both molecules. The infrared part of the spectrum was calibrated using lines of HF impurity [22]. The accuracy of the measured lines is estimated to vary from ±0.002 to ±0.01 cm^{-1}, depending on the S/N ratio.

3. Experimental results

For the $A'^3\Phi_4 \rightarrow X^3\Phi_4$ transition of CoH, the (2,0), (1,0), (0,0), (0,1), and (1,2) bands were assigned. For the $v'' = 0$ level, the lines were followed up to $J''_e = 26$ for the

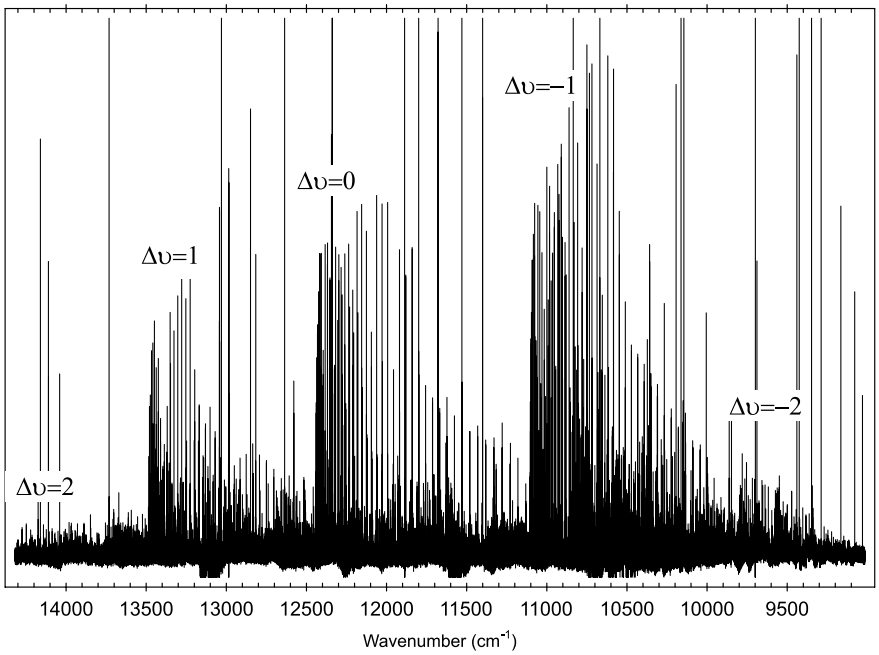

Fig. 1. An overview spectrum of CoD after baseline correction.

e-parity component and to $J''_f = 33$ for the *f*-parity component; for $v'' = 1$ they were followed up to $J''_e = 26$ and $J''_f = 31$, and for $v'' = 2$ up to $J''_e = 21$ and $J''_f = 18$. For the corresponding transition of CoD the (2,0), (1,0), (2,1), (0,0), (0,1), (1,2), (2,3), (0,2), and (1,3) bands were analyzed. Assignments were made up to $J''_e = J''_f = 37$ for $v'' = 0$ and 1, up to $J''_e = J''_f = 22$ for $v'' = 2$, and up to $J''_e = J''_f = 16$ for $v'' = 3$. For the $A'^3\Phi_3 \rightarrow X^3\Phi_3$ transitions of both CoH and CoD and for the $[13.3]4 \rightarrow X^3\Phi_3$ and $[13.3]4 \rightarrow X^3\Phi_4$ transitions of CoD, only the (0,0) bands were observed. However, both the (0,0) and (0,1) bands were analyzed for the $A'^3\Phi_3 \rightarrow X^3\Phi_4$ system of CoH. For the $\Omega'' = 3$ component, lines were found corresponding to *J*'s up to $J''_e = 16$ and $J''_f = 23$ for CoH, and up to $J''_e = J''_f = 21$ for CoD.

In all transitions with $\Delta\Omega = 0$, *P* and *R* branches appear to have similar relative intensities, while *Q* branches disappear rapidly with increasing *J*. In the $[13.3]4 \rightarrow X^3\Phi_4$ transition in CoD, the lines start to appear only for $J \geqslant 13$, and the *Q* branch was not observed. In the $[13.3]4 \rightarrow X^3\Phi_3$ transition, the *P* branch is much weaker than the *R* and *Q* branches. In addition, the overall intensity of this band is weaker than that of the $[13.3]4 \rightarrow X^3\Phi_4$ transition. These observations were the basis of our conclusion that $\Omega' = 4$ for the upper state of this transition.

The $A'^3\Phi_3 \rightarrow X^3\Phi_4$ transition of CoH has strong *R* and *Q* branches, but the *P* branch is so weak that we were only able to assign two *P* lines. This is not the pattern one would expect for a transition with $\Delta\Omega = -1$, for which the *P* branch should be stronger than the *R* branch, but strong interactions between close-lying states in CoH may be responsible for this unexpected intensity pattern. Most of the recorded bands are also severely perturbed, especially the ones originating in the [13.3]4 state of CoD. The assignments of the lines were made by the application of combination differences starting from assignments for the ground states of CoD and CoH known from the previous experimental work [4,11]. We were unable to find transitions to the $\Omega'' = 2$ component of the ground state, probably because it is extremely perturbed, as was suggested in [11]. There are many unassigned lines in the spectra of both isotopologues. The most intense unassigned bands are in the 7500–8500 cm^{-1} region; it is unclear what states are involved in these transitions, but they are certainly not known states.

Because the spectroscopic constants for $\Omega = 3$ and $\Omega = 4$ spin components in the ground and excited electronic states are quite different, it was decided to use empirical Hund's case (c) expressions when fitting the data. We have performed band-constant and Dunham-type expansion fits for CoH and CoD separately, as well as a combined-isotopologue Dunham-expansion fit, all using program DPARFIT 3.3 [23]. An experimental uncertainty of ± 0.007 cm^{-1} was assigned to most of the lines. The data of Heimer [1] and of Klynning and Kroneqvist [4,5] were included in our fit (with ± 0.04 and ± 0.03 cm^{-1} uncertainties, respectively) to obtain a consistent set of spectroscopic constants. However, some of their published lines were omitted from the analysis because of discrepancies in the combination differences.

4. Data analysis

In the present work, the quality of a fit of *N* data $y_{obs}(i)$ with associated uncertainties $u(i)$ is indicated by the value of the dimensionless root mean square deviation ($\overline{dd}$),

$$\overline{dd} \equiv \left\{ \frac{1}{N} \sum_{i=1}^{N} \left[\frac{y_{\mathrm{calc}}(i) - y_{\mathrm{obs}}(i)}{u(i)} \right]^2 \right\}^{1/2}, \quad (1)$$

in which $y_{\mathrm{calc}}(i)$ is the value of datum-i calculated from the model. In all of our fits for determining ground-state parameters, the levels of the severely perturbed excited electronic states were represented by independent term values.

In our band-constant treatment of the ground state, its level energies were represented by the following Hund's case (c) expression:

$$\begin{aligned} F_v(J) = T_v &+ B_v[J(J+1) - \Omega^2] - D_v[J(J+1) - \Omega^2]^2 \\ &+ H_v[J(J+1) - \Omega^2]^3 + L_v[J(J+1) - \Omega^2]^4 \\ &\pm \frac{1}{2}[J(J+1)]^{\Omega} \sum_{m=\Omega} q_m [J(J+1) - \Omega^2]^{m-\Omega} \end{aligned} \quad (2)$$

The form of the last term in this equation reflects the fact that the magnitude of Ω-doubling splittings increases as $\sim J^{2\Omega}$ [24]. In particular, it implies that if $\Omega = 3$ then the leading Ω-doubling splitting term is $q_H[J(J+1)]^3$, while if $\Omega = 4$ it would be $q_L[J(J+1)]^4$. Note that following common practice, the m-subscript in our tabulated values of q is replaced by the label for the mechanical rotational constant of the same order in $J(J+1)$.

It is interesting to note that the quality of fit can provide a very sharp means of determining the correct value of Ω for the state in question. For example, fits of Eq. (2) to the data for the (0,0) band of the $A'^3\Phi_4 \rightarrow X^3\Phi_4$ transition of CoH using different assumed values of the total electronic angular momentum quantum number Ω in Eq. (2) gave the results shown in Fig. 2. Note that only the leading ($m = \Omega$) term in the Ω-doubling expansion was used in these fits, and the number of rotational constants was always the same. The well-defined minimum in that plot clearly shows that $\Omega = 4$ for the lower state of this band.

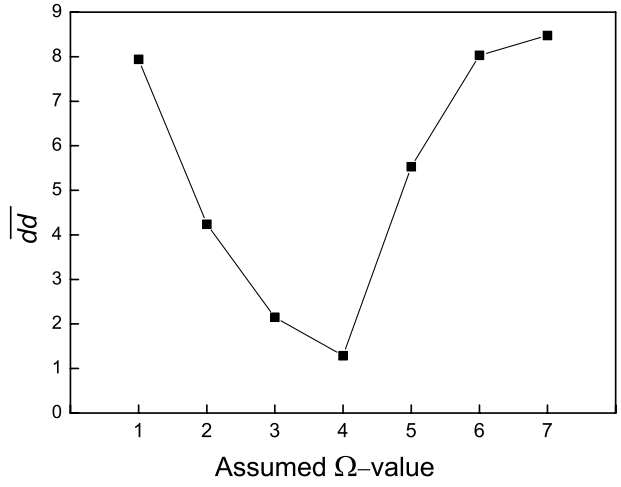

Fig. 2. For a fit to the (0,0) band of the $A'^3\Phi_4 \rightarrow X^3\Phi_4$ transition of CoH, the dependence of the quality of fit on the assumed value of the total angular momentum quantum number Ω determining the leading power of $[J(J+1)]$ in the Ω-doubling term in the last row of Eq. (2).

The $v = 1$ vibrational level of the $X^3\Phi_4$ sub-state appears to be slightly perturbed between $J'' = 13$ and $J'' = 21$; therefore, larger uncertainties were assigned to these lines. Despite the fact that $v = 2$ state fits well, it is probably slightly perturbed as well, because the values of its constants do not follow the trend established by $v = 0$ and 1.

The results of our band-constant fits for CoH ($\overline{dd} = 1.007$) and CoD ($\overline{dd} = 0.9964$) are presented in Table 1. The output files from program DPARFIT 3.3 listing the experimental line positions and fitted term values for the excited electronic states are available on ScienceDirect.

In a second stage of the analysis, the ground-state constants were held fixed at the values shown in Table 1 while the upper-state levels were fitted to Eq. (2). Since all the upper states are heavily perturbed, we used the "robust" option of program DPARFIT, which applies Watson's [25] iterative "robust" procedure for minimizing the effect on the fit of contributions from lines with large discrepancies from the model. This approach worked fairly well for CoD, but required some "manual" help for CoH; i.e., some lines had to be assigned larger uncertainties before performing the fit. The resulting constants obtained for the excited electronic states are listed in Tables 2 and 3. The large differences between the B_v values for the $A'^3\Phi_4$ and $A'^3\Phi_3$ spin components show that the Ω-components of these excited state are mixed with the sub-states of other electronic states, and confirms that the use of Hund's case (c) expressions is justified, i.e., that these Ω-components can be treated as independent electronic states.

Since the ground $X^3\Phi_4$ state appears to be only slightly perturbed, it seemed appropriate to perform a combined-isotopologue fit to the data for CoH and CoD together. Following the formalism of [26,27], the level energies were represented by the expression

$$\begin{aligned} E^{(\alpha)}(v,J) = &\sum_{m=0} \sum_{l=0} \left\{ Y_{l,m}^{(\mathrm{CoH})} + \frac{\Delta M_{\mathrm{H}}^{(\alpha)}}{M_{\mathrm{H}}^{(\alpha)}} \delta_{l,m}^{\mathrm{H}} \right\} \left(\frac{\mu_{\mathrm{CoH}}}{\mu_\alpha} \right)^{m+l/2} \\ &\times \left(v + \frac{1}{2}\right)^l \left[J(J+1) - \Omega^2\right]^m \pm \frac{1}{2}[J(J+1)]^{\Omega} \sum_{m=\Omega} \\ &\times \sum_{l=0} q_{l,m}^{(\mathrm{CoH})} \left(\frac{\mu_{\mathrm{CoH}}}{\mu_\alpha} \right)^{\Omega+m+l/2} \times \left(v + \frac{1}{2}\right)^l [J(J+1) - \Omega^2]^{m-\Omega}, \end{aligned} \quad (3)$$

in which α labels a particular isotopologue and $\Delta M_{\mathrm{A}}^{(\alpha)}$ is the difference between the atomic mass of atom A in isotopologue-α and in the reference isotopologue, which was chosen to be CoH. Since Co has only one naturally occurring isotope, no Co atom Born–Oppenheimer breakdown (BOB) coefficients ($\delta_{l,m}^{\mathrm{Co}}$) appear in Eq. (3). The Dunham-type parameters $Y_{l,m}^{(\mathrm{CoH})}$ and $q_{l,m}^{(\mathrm{CoH})}$ which characterize the CoH isotopologue are directly determined by the fit, while the analogous parameters for the deuteride species are readily obtained by taking account of mass scaling and contributions from the BOB terms:

Table 1
Spectroscopic constants (in cm^{-1}) for the $X^3\Phi_4$ and $X^3\Phi_3$ states of CoH and CoD

v	T_v	B_v	$-10^4\ D_v$	$10^9\ H_v$	$10^{11}\ L_v$	$10^8\ q_H$	$10^{11}\ q_L$	$10^{14}\ q_M$
CoH $X^3\Phi_4$								
0	0.0	7.136591(160)	−4.0096(93)	8.4(2.1)	−1.34(12)	—	−1.167(100)	−0.87(15)
1	1855.3720(64)	6.925110(180)	−4.0672(97)	33.8(2.0)	−3.47(14)	—	2.37(97)	−5.09(13)
2	3641.603(95)	6.71168(38)	−3.948(42)	61.(18)	−18.7(2.6)	—	1.3(1.3)	31.(41)
CoH $X^3\Phi_3$								
0	675.564(14)	7.27614(21)	−5.3253(79)	−8.6290(130)	—	−169.32(25)		
CoD $X^3\Phi_4$								
0	0.0	3.719474(59)	−1.11330(110)	1.65(53)	—	—	−0.00900 (110)	
1	1338.0940(40)	3.641032(64)	−1.10797(120)	1.68(61)	—	—	−0.01870(120)	
2	2640.9270(52)	3.56283(16)	−1.08400(180)	—	—	—	−0.170(55)	
3	3908.6000(120)	3.48426(20)	−1.0690(72)	—	—	—	−0.30(37)	
CoD $X^3\Phi_3$								
0	669.045(50)	3.75536(54)	−1.1792(230)	−7.9(4.0)	−3.56(27)	−0.437(110)	8.20(26)	

The numbers in parentheses are 95% confidence limit uncertainties (approximately two standard deviations) in units of the last significant digit quoted.

Table 2
Spectroscopic constants (in cm^{-1}) for the excited states of CoH. Uncertainties are defined as in Table 1

v	T_v	B_v	$-10^4\ D_v$	$10^6\ H_v$	$10^8\ L_v$	$10^7\ q_H$	$10^9\ q_L$	$10^{11}\ q_M$
CoH $A'^3\Phi_4$								
0	12358.4390(85)	5.47693(69)	4.28(14)	1.760(73)	—	—	10.03(39)	−8.30(35)
1	13796.574(13)	5.28919(190)	3.68(66)	9.33(75)	−6.20(24)	—	5.32(55)	−3.10(28)
2	15136.047(150)	5.1564(40)	−8.43(33)	6.04(85)	—	—	4.72(99)	−2.010(53)
CoH $A'^3\Phi_3$								
0	12644.977(18)	6.36226(49)	−10.6810(43)	0.826(11)	—	−5.380(68)	1.580(32)	
CoH $A^3\Phi_4$[a]								
0	22243.210(43)	6.5197(14)	−5.260(74)	−0.035(16)	—	—	−0.06(2)	

[a] These constants are calculated using the line lists from [1].

Table 3
Spectroscopic constants (in cm^{-1}) for the excited states of CoD. Uncertainties are defined as in Table 1

v	T_v	B_v	$-10^4\ D_v$	$10^7\ H_v$	$10^9\ L_v$	$10^8\ q_H$	$10^{10}\ q_L$	$10^{13}\ q_M$
CoD $A'^3\Phi_4$								
0	12415.6620(37)	2.935920(64)	−0.3863(270)	−0.2731(40)	0.01240(18)	—	0.01547(83)	−0.0082(69)
1	13460.6260(100)	2.90166(53)	0.689(73)	−5.37(30)	1.230(38)	—	−0.942(110)	−3.40(31)
2	14459.2060(81)	2.87454(27)	0.469(31)	2.100(90)	—	—	0.0	—
CoD $A'^3\Phi_3$								
0	12687.207(250)	3.22093(54)	−8.166(38)	20.44(11)	−1.900(110)	4.07(45)	−2.00(12)	
CoD [13.3]4								
0	13293.008(160)	3.6180(15)	−14.833(48)	13.951(69)	−0.5988(39)	—	−1.6909(15)	2.640(22)
CoD $A^3\Phi_4$[a]								
0	22267.480(18)	3.34007(46)	−1.076(29)	−0.520(61)	0.0460(40)	—	−0.0130(12)	
1	23383.261(22)	3.23602(67)	−0.776(58)	−2.06(19)	0.240(20)	—	1.824(11)	−3.90(21)
2	24433.450(86)	3.1212(51)	−2.010(97)	15.(10)	—	—	−110(52)	
CoD $A^3\Phi_3$[a]								
0	22598.221(19)	3.37874(38)	−1.291(18)	0.050(21)	—	1.23(21)	−0.760(36)	
1	23708.644(25)	3.27127(64)	−1.208(41)	−0.210(68)	—	−1.60(11)		

[a] These constants are calculated using the line lists from [4] and [5].

$$Y_{l,m}^{(\mathrm{CoD})} = \left\{ Y_{l,m}^{(\mathrm{CoH})} + \frac{M_\mathrm{D} - M_\mathrm{H}}{M_\mathrm{H}} \delta_{l,m}^{\mathrm{H}} \right\} \left(\frac{\mu_\mathrm{CoH}}{\mu_\mathrm{CoD}} \right)^{m+l/2}, \quad (4)$$

$$q_{l,m}^{(\mathrm{CoD})} = q_{l,m}^{(\mathrm{CoH})} \left(\frac{\mu_\mathrm{CoH}}{\mu_\mathrm{CoD}} \right)^{\Omega+m+l/2}. \quad (5)$$

The results of this fit are presented in Table 4. A relatively large number (eight!) of Born–Oppenheimer breakdown parameters $\delta_{l,m}^{\mathrm{H}}$ was required, and their values are relatively large, which is often the case for metal hydrides [28]. This fit was also carried out using the "robust" option of DPARFIT because of the perturbations in CoH.

A Dunham-type fit was also carried out using Eq. (3) (without the BOB terms) for each isotopologue separately, because the $X^3\Phi_4$ state of CoH is slightly perturbed for $v = 1$ and 2, and this definitely affected the combined-isotopologue fit. The results of those independent Dunham-type fits are presented in Table 5. The equilibrium bond lengths for CoH and CoD, calculated using the $Y_{0,1}$ values in Table 4, were found to be $r_e = 1.532664(16)$ and 1.517531(29) Å, respectively. The (approximately) 1% difference between the r_e values of the two isotopologues is due to the breakdown of the Born–Oppenheimer approximation and to the effect of perturbations.

Table 4
Dunham-type parameters and Born–Oppenheimer breakdown parameters (in cm^{-1}) for the $X^3\Phi_4$ state of CoH determined from the combined-isotopologue analysis. Uncertainties are defined as in Table 1

Constant	CoH	CoD
$\tilde{T}_{v=-1/2}$	953.730825	682.294956
$Y_{1,0}$	1924.8598(230)	1373.4397(140)
$Y_{2,0}$	−34.8214(150)	−17.7087(73)
$10^2 \times Y_{3,0}$	5.02(32)	1.821(120)
$Y_{0,1}$	7.242385(74)	3.758673(73)
$Y_{1,1}$	−0.212336(270)	−0.078031(82)
$10^4 \times Y_{2,1}$	2.87(99)	−0.67(26)
$10^4 \times Y_{0,2}$	−3.9856(83)	−1.1132(23)
$10^6 \times Y_{1,2}$	0.210(94)	−2.11(21)
$10^6 \times Y_{2,2}$	−2.11(25)	0.656(66)
$10^8 \times Y_{0,3}$	−0.672(170)	0.188(24)
$10^8 \times Y_{1,3}$	2.188(130)	0.2055(120)
$10^{13} \times Y_{0,4}$	−10(13)	−0.67(89)
$10^{11} \times Y_{1,4}$	−1.910(100)	−0.0913(49)
$q_{0,4}$	$-0.56(11) \times 10^{-11}$	$-2.36(47) \times 10^{-15}$
$q_{1,4}$	$-3.278(180) \times 10^{-11}$	$-1.220(67) \times 10^{-16}$
$q_{2,4}$	$3.370(70) \times 10^{-11}$	$1.107(23) \times 10^{-18}$
$q_{0,5}$	$1.440(130) \times 10^{-14}$	$4.18(39) \times 10^{-24}$
$q_{1,5}$	$-4.120(98) \times 10^{-14}$	$-1.054(25) \times 10^{-25}$
$\delta_{1,0}^{\mathrm{H}}$	1.273(32)	
$10^3 \times \delta_{2,0}^{\mathrm{H}}$	0.310(130)	
$10^1 \times \delta_{0,1}^{\mathrm{H}}$	2.90555(34)	
$10^3 \times \delta_{1,1}^{\mathrm{H}}$	−5.36(47)	
$10^3 \times \delta_{2,1}^{\mathrm{H}}$	−1.10(23)	
$10^5 \times \delta_{0,2}^{\mathrm{H}}$	−6.303(110)	
$10^5 \times \delta_{1,2}^{\mathrm{H}}$	−2.330(150)	
$10^5 \times \delta_{2,2}^{\mathrm{H}}$	1.420(97)	
$10^8 \times \delta_{0,3}^{\mathrm{H}}$	4.200(100)	

Table 5
Dunham-type parameters for the $X^3\Phi_4$ state of CoH and CoD, all in cm^{-1}. Uncertainties are defined as in Table 1

Constant	CoH	CoD
$\tilde{T}_{v=-1/2}$	953.6188875	682.303188
$Y_{1,0}$	1924.5256(21)	1373.4556(150)
$Y_{2,0}$	−34.5757(76)	−17.7063(86)
$10^2 \times Y_{3,0}$	—	1.570(140)
$Y_{0,1}$	7.24175(26)	3.758823(69)
$10 \times Y_{1,1}$	−2.0984(42)	−0.78765(52)
$10^3 \times Y_{2,1}$	−0.851(160)	0.1480(120)
$10^4 \times Y_{0,2}$	−3.9069(140)	−1.11661(120)
$10^5 \times Y_{1,2}$	−2.618(210)	0.0625(69)
$10^5 \times Y_{2,2}$	1.045(79)	—
$10^8 \times Y_{0,3}$	−2.287(30)	0.168(63)
$10^8 \times Y_{1,3}$	7.697(35)	−0.0030(39)
$10^8 \times Y_{2,3}$	−2.640(120)	—
$10^{12} \times Y_{0,4}$	−3.8(2.2)	—
$10^{11} \times Y_{1,4}$	−2.03(15)	—
$10^{11} \times q_{0,4}$	0.349(170)	0.0039(11)
$10^{11} \times q_{1,4}$	−5.118(24)	−0.00970(57)
$10^{11} \times q_{2,4}$	−4.300(93)	—
$10^{14} \times q_{0,5}$	1.14(21)	—
$10^{14} \times q_{1,5}$	−4.130(150)	—
$\overline{dd}$	1.058	1.040

5. Discussion

When comparing our spectroscopic constants with those derived in previous experimental work [1,3–11], one has to be very cautious because of the different energy level expressions used. For instance, band origins for the excited $A'^3\Phi_4$ state reported by Barnes et al. [10] and Ram et al. [11] differ by as much as $\sim 30\ \mathrm{cm}^{-1}$. However, this is merely because Ram et al. [11] did not include the term Ω^2 in the rotational angular momentum factor $[J(J+1) - \Omega^2]$ in their versions of Eq. (2).

One can compare values of the spin–orbit splitting in the ground state obtained in this work with values determined in the laser experiments [8,10]. If one considers the ground-state term values of CoH calculated using constants from Table 1, the difference between the energy levels $J = 4$ in $\Omega = 3$ and $J = 4$ in $\Omega = 4$ is found to be $726.996\ \mathrm{cm}^{-1}$, which is in excellent agreement with the value of $728(\pm 3)\ \mathrm{cm}^{-1}$ reported in [8]. However, for CoD our difference between $J = 4$ in $\Omega = 3$ and $J = 4$ in $\Omega = 4$ levels is found to be $695.464\ \mathrm{cm}^{-1}$, which is significantly different from the value of $729(\pm 2)\ \mathrm{cm}^{-1}$ reported by Barnes et al. [10]. The reason for this discrepancy is not yet understood.

Our parity assignments are based on the following arguments. The fact that only one parity component of the $X^3\Phi_3$ state of the CoH molecule is perturbed leads to the assumption that the perturbing state has only one parity component. The ab initio calculations of [18] predict that a $^3\Sigma^-$ state lies only 0.14 eV above the ground electronic state. This state has a 0^+ spin component of e-parity, and we believe that despite the difference in Ω values, it is a perturber of the $X^3\Phi_3$ state. That means that the perturbed

levels must belong to the *e*-parity component, and this makes it possible to assign the parities of all observed energy levels in the ground and excited electronic states. This in turn means that the tentative parity assignments reported in [11] have to be changed. Also one can assume that the 0^+ spin component of the $^3\Sigma^-$ state is located ~700 cm^{-1} (based on the spin–orbit splitting in the ground state) above the $X^3\Phi_4$ state. Nevertheless, it should be noted that since the *e* and *f* levels of the same *J* for the $\Omega = 1$ component of the $^3\Sigma^-$ state are widely separated, one of those components could also be responsible for perturbing only one parity component of the $X^3\Phi_3$ sub-state.

The anomalous broadening of the high *J* lines of the transitions terminating on the $X^3\Phi_3$ state that was observed in this work was also noticed by Klynning and Kroneqvist [5] in the $A^3\Phi_3$–$X^3\Phi_3$ transition of CoH. They suggested that it may be caused by predissociation of the upper state. However, the experiments in [5] were done in absorption, and since we are observing the same broadening in emission it is unlikely that it is caused by predissociation. It is more likely that this broadening is due to hyperfine perturbations, which were also observed in the $X^3\Phi_3$ state of CoCl by Flory et al. [29]. In the case of CoCl, it was suggested that these perturbations are caused by second-order spin–orbit mixing with a nearby isoconfigurational $^1\Phi_3$ state, but theoretical predictions [18] suggest that for the CoH molecule the $^1\Phi$ state is located 2.60 eV above the ground state; therefore, it cannot be responsible for the hyperfine perturbations.

The [13.3]4 state of CoD observed in this work is most probably a $^1\Gamma_4$ state, as it is the only state within 5000 cm^{-1} of the $A'^3\Phi$ state that is predicted to have an $\Omega = 4$ spin component [18]. Fig. 3 illustrates electronic states of the CoH molecule observed in all previous optical experiments to date. The transitions observed in this work are marked with arrows.

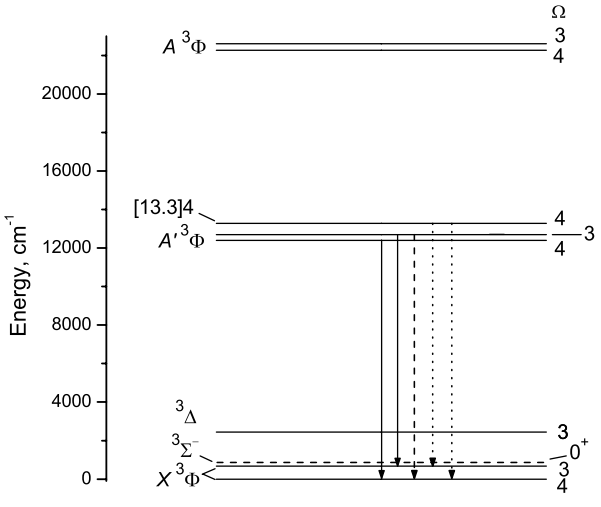

Fig. 3. Energy level diagram showing the electronic states found in [1,3–11] and in the present work. The transitions observed here are marked with arrows: solid arrows label transitions observed for both CoH and CoD, dashed arrows label only CoH, and dotted arrows label only CoD transitions.

6. Conclusions

The Fourier transform emission spectra of CoH and CoD have been investigated in the near infrared region. A detailed analysis of bands of the $A'^3\Phi \rightarrow X^3\Phi$ transitions in both molecules has provided an improved set of ground-state band-constants and Dunham-type constants for the $\Omega = 4$ component of both CoH and CoD. A combined-isotopologue fit was also performed to the data for the $X^3\Phi_4$ spin component. That global fit of all transitions (including those from the previous optical experiments) has provided more precise values for the spin–orbit splittings between $\Omega = 4$ and $\Omega = 3$ in the ground and excited electronic states. We find no trace of any spin components with $\Omega = 2$. This is probably due to the fact that these sub-states are more perturbed than those with higher Ω values because there are more possible perturbers, as predicted by the ab initio calculations of [18].

Acknowledgment

Financial support from the Natural Sciences and Engineering Research Council of Canada is gratefully acknowledged.

Appendix A. Supplementary data

Supplementary data for this article are available on ScienceDirect (www.sciencedirect.com) and as part of the Ohio State University Molecular Spectroscopy Archives (http://msa.lib.ohio-state.edu/jmsa_hp.htm).

References

[1] A. Heimer, Z. Phys. 104 (1937) 448–457.
[2] G. Herzberg, Molecular Spectra and Molecular Structure I, Diatomic molecules, Van Nostrand, New Jersey, 1953.
[3] L. Klynning, H. Neuhaus, Zes. Naturforsch A 18 (1963) 1142.
[4] L. Klynning, M. Kroneqvist, Phys. Scr. 6 (1972) 61–65.
[5] L. Klynning, M. Kroneqvist, Phys. Scr. 7 (1973) 72–74.
[6] L. Klynning, M. Kroneqvist, Phys. Scr. 24 (1981) 21–22.
[7] R.E. Smith, Proc. R. Soc. London A322 (1973) 113–127.
[8] T.D. Varberg, E.J. Hill, R.W. Field, J. Mol. Spectrosc. 138 (1989) 630–637.
[9] T.D. Varberg, Ph. D. Thesis, MIT, Cambridge, MA, 1992.
[10] M. Barnes, A.J. Merer, G.F. Metha, J. Mol. Spectrosc. 173 (1995) 100–112.
[11] R.S. Ram, P.F. Bernath, S.P. Davis, J. Mol. Spectrosc. 175 (1996) 1–6.
[12] A.E.S. Miller, C.S. Feigerle, W.C. Lineberger, J. Chem. Phys. 87 (1987) 1549–1556.
[13] K. Lipus, T. Nelis, E. Bachem, W. Urban, Mol. Phys. 68 (1989) 1171–1177.
[14] S.P. Beaton, K.M. Evenson, T. Nelis, J.M. Brown, J. Chem. Phys. 89 (1988) 4446–4448.
[15] S.P. Beaton, K.M. Evenson, J.M. Brown, J. Mol. Spectrosc. 164 (1994) 395–415.
[16] D.P. Chong, S.R. Langhoff, C.W. Bauschlicher Jr., S.P. Walch, H. Partridge, J. Chem. Phys. 85 (1986) 2850–2860.

[17] Anglada, P.J. Bruna, F. Grein, J. Chem. Phys. 92 (1990) 6732–6747.
[18] M. Freindorf, C.M. Mariam, B.A. Hess, J. Chem. Phys. 99 (1993) 1215–1223.
[19] V. Barone, C. Adamo, Int. J. Quantum Chem. 61 (1997) 443–451.
[20] N.E. Schultz, Y. Zhao, D.G. Truhlar, J. Phys. Chem. A 109 (2005) 11127–11143.
[21] T. Hirano, private communication.
[22] R.B. LeBlanc, J.B. White, P.F. Bernath, J. Mol. Spectrosc. 164 (1994) 574–579.
[23] R.J. Le Roy, DParFit 3.3, A Computer Program for Fitting Multi-Isotopomer Diatomic Molecule Spectra, University of Waterloo Chemical Physics Research Report CP-660, 2005; <http://leroy.uwaterloo.ca/>.
[24] J.M. Brown, A. Carrington, Rotational Spectroscopy of Diatomic Molecules, Cambridge University Press, Cambridge, UK, 2003.
[25] J.K.G. Watson, J. Mol. Spectrosc. 219 (1999) 326–328.
[26] R.J. Le Roy, J. Mol. Spectrosc. 194 (1999) 189–196.
[27] Y. Huang, R.J. Le Roy, J. Chem. Phys. 119 (2003) 7398–7416.
[28] A. Shayesteh, D.R.T. Appadoo, I. Gordon, R.J. Le Roy, P.F. Bernath, J. Chem. Phys. 120 (2004) 10002–10008.
[29] M.A. Flory, D.T. Halfen, L.M. Ziurys, J. Chem. Phys. 121 (2004) 8385–8392.